

PLUS package. Crystal data, details of the data collection, and structure analysis are summarized in Table V. For all structures, all nonhydrogen atoms were refined with anisotropic parameters. All hydrogen atoms included in the structure factor calculations were placed in idealized positions.

Acknowledgment. We thank the National Science Council of

the Republic of China for financial support of this work.

Supplementary Material Available: Crystal data and full tables of bond lengths and angles and final atomic coordinates (14 pages); observed and calculated structural factors for **2b**, **2e**, and **6b** (25 pages). Ordering information is given on any current masthead page.

Molecular Semiconductors from Bifunctional Dithia- and Diselenadiazolyl Radicals. Preparation and Solid-State Structural and Electronic Properties of 1,4-[(E₂N₂C)C₆H₄(CN₂E₂)] (E = S, Se)

A. Wallace Cordes,^{1a,*} Robert C. Haddon,^{1b,*} Richard T. Oakley,^{*1c} Lynn F. Schneemeyer,^{1b} Joseph V. Waszczak,^{1b} Kelly M. Young,^{1c} and Neil M. Zimmerman^{1b}

Contribution from the Department of Chemistry and Biochemistry, University of Arkansas, Fayetteville, Arkansas 72701, AT&T Bell Laboratories, Murray Hill, New Jersey 07974, and Guelph Waterloo Centre for Graduate Work in Chemistry, Guelph Campus, Department of Chemistry and Biochemistry, University of Guelph, Guelph, Ontario N1G 2W1, Canada. Received June 7, 1990

Abstract: The reactions of 1,4-phenylenebis[*N,N,N'*-tris(trimethylsilyl)amidine] with sulfur and selenium dichlorides yield, respectively, the 1,4-phenylenebis(dithiadiazolium) and bis(diselenadiazolium) dichlorides 1,4-[(E₂N₂C)C₆H₄(CN₂E₂)]Cl₂ (E = S, Se). Reduction of these materials with triphenylantimony affords the corresponding diradical species 1,4-[(E₂N₂C)C₆H₄(CN₂E₂)], which can be purified by high vacuum sublimation. The crystal structures of 1,4-[(E₂N₂C)C₆H₄(CN₂E₂)] (E = S, Se) are both monoclinic, space group *P2₁/n*. The crystal packing consists of sheets of interleaved columns of weakly associated diradical units (dimers); the mean intradimer separation is 3.34/3.37 Å (E = S/Se), and the mean interdimer separation is 3.68/3.71 Å (E = S/Se). The sulfur compound is an insulator, but the selenium material has a room temperature pressed pellet resistivity of about 100 Ω cm. Magnetic susceptibility measurements show the solids to be predominantly diamagnetic with variable amounts of paramagnetic defects in the lattice. While the exact mechanism of conduction remains to be established, these systems represent the first structurally characterized conducting materials constructed from neutral molecular radicals. Extended Hückel band structure calculations reveal band gaps of 0.84/0.69 eV (E = S, Se) for the crystalline solids. The calculated band dispersions show a high degree of three-dimensionality; to our knowledge these are the most isotropic organic molecular solids yet to be reported.

Introduction

Research into the development of low-dimensional molecular conductors and superconductors has focused heavily on the use of charge-transfer salts,² e.g., TTF TCNQ, or radical ion (Bechgaard) salts such as those based on the TMTSF and BEDT-TTF donors.³ Conductivity in these materials depends on efficient overlap between the π -systems of the molecular building blocks, which are often stacked in uniform one-dimensional columns. The susceptibility of these columns to undergo a Peierls distortion⁴ with consequent loss of conductivity requires designing structures in which intercolumnar interactions are optimized. Considerable effort has therefore been directed toward modifying both the size and shape of the counterion.

An alternative approach to molecular conductors, one which obviates the need for counterions, involves the use of neutral rather

than charged π -radicals. Several variations⁵ on the originally proposed phenalenyl framework⁶ have been pursued, but a paucity of structural data has hindered progress. Recent advances in heterocyclic sulfur nitrogen chemistry,⁷ however, particularly the characterization of a number of stable radical systems,⁸ have

(1) (a) University of Arkansas. (b) AT&T Bell Laboratories. (c) University of Guelph.

(2) See, for example: (a) Garito, A. F.; Heeger, A. J. *Acc. Chem. Res.* **1974**, *7*, 232. (b) Torrance, J. B. *Acc. Chem. Res.* **1979**, *12*, 79. (c) Perlstien, J. H. *Angew. Chem., Int. Ed. Engl.* **1977**, *16*, 519.

(3) (a) Wudl, F. *Acc. Chem. Res.* **1984**, *17*, 227. (b) Williams, J. M.; Beno, M. A.; Wang, H. H.; Leung, P. C. W.; Emge, T. J.; Geiser, U.; Carlson, K. D. *Acc. Chem. Res.* **1985**, *18*, 261. (c) Williams, J. M.; Wang, H. H.; Emge, T. J.; Gieser, U.; Beno, M. A.; Leung, P. C. W.; Carlson, K. D.; Thorn, R. J.; Schultz, A. J.; Whangbo, M.-H. *Prog. Inorg. Chem.* **1987**, *35*, 51. (d) Inokuchi, H. *Angew. Chem., Int. Ed. Engl.* **1988**, *27*, 1747.

(4) Peierls, R. E. *Quantum Theory of Solids*; Oxford, London, 1953; p 108.

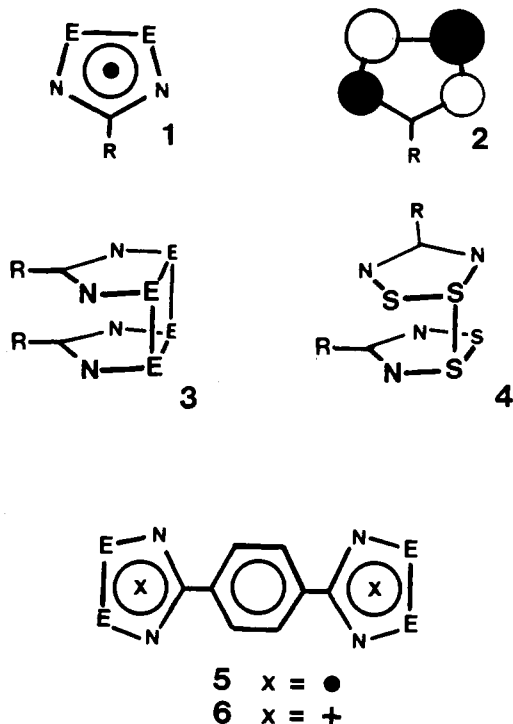
(5) (a) Haddon, R. C.; Wudl, F.; Kaplan, M. L.; Marshall, J. H.; Cais, R. E.; Bramwell, F. B. *J. Am. Chem. Soc.* **1978**, *100*, 7629. (b) Kaplan, M. L.; Haddon, R. C.; Hirani, A. M.; Schilling, F. C.; Marshall, J. H. *J. Org. Chem.* **1981**, *47*, 675. (c) Haddon, R. C.; Chichester, S. V.; Stein, S. M.; Marshall, J. H.; Muijsce, A. M. *J. Org. Chem.* **1987**, *52*, 711. (d) Canadell, E.; Shaik, S. S. *Inorg. Chem.* **1987**, *26*, 3797. (e) Nakasuji, K.; Yamaguchi, M.; Murata, I.; Yamaguchi, K.; Fueno, T.; Ohya-Nishiguchi, H.; Sugano, T.; Kinoshito, M. *J. Am. Chem. Soc.* **1989**, *111*, 9265.

(6) (a) Haddon, R. C. *Nature (London)* **1975**, *256*, 394. (b) Haddon, R. C. *Aust. J. Chem.* **1975**, *28*, 2343.

(7) Oakley, R. T. *Prog. Inorg. Chem.* **1988**, *36*, 299.

(8) (a) Wolmershäuser, G.; Schnauber, M.; Wilhelm, T. *J. Chem. Soc., Chem. Commun.* **1984**, 573. (b) Wolmershäuser, G.; Schnauber, M.; Wilhelm, T.; Sutcliffe, L. H. *Synth. Met.* **1986**, *14*, 239. (c) Dormann, E.; Nowak, M. J.; Williams, K. A.; Angus, R. O., Jr.; Wudl, F. *J. Am. Chem. Soc.* **1987**, *109*, 2594. (d) Wolmershäuser, G.; Wortmann, G.; Schnauber, M. *J. Chem. Res. Synop.* **1988**, 358. (e) Wolmershäuser, G.; Johann, R. *Angew. Chem., Int. Ed. Engl.* **1989**, *28*, 920. (f) Hayes, P. J.; Oakley, R. T.; Cordes, A. W.; Pennington, W. T. *J. Am. Chem. Soc.* **1985**, *107*, 1346. (g) Boeré, R. T.; Cordes, A. W.; Hayes, P. J.; Oakley, R. T.; Reed, R. W. *Inorg. Chem.* **1986**, *25*, 2445. (h) Oakley, R. T.; Reed, R. W.; Cordes, A. W.; Craig, S. L.; Graham, J. B. **1987**, *109*, 7745. (i) Boeré, R. T.; French, C. L.; Oakley, R. T.; Cordes, A. W.; Privett, J. A. J.; Craig, S. L.; Graham, J. B. *J. Am. Chem. Soc.* **1985**, *107*, 7710. (j) Awere, E. G.; Burford, N.; Haddon, R. C.; Parsons, S.; Passmore, J.; Waszczak, J. V.; White, P. S. *Inorg. Chem.* In press. (k) Wolmershäuser, G.; Kraft, G. *Chem. Ber.* **1990**, *123*, 881.

prompted us to investigate the use of thiazyl radicals as molecular building blocks. Within this context the 7π -electron 1,2,3,5-dithiadiazolyl radical **1** ($E = S$) represents an attractive candidate.⁹ ESR,^{9b-d,f} photoelectron,^{9d,f} and theoretical^{9b-d,f} studies on derivatives of this type reveal an electronic structure in which the unpaired electron is confined to the a_2 distribution **2**. The nodal plane of this SOMO effectively restricts spin leakage onto the ligands; hyperfine coupling constants and ionization potentials are consequently relatively invariant to substituent effects. Quantitative ESR measurements on solutions of **1** ($E = S$, $R = Ph$) in toluene indicate an enthalpy of association near 35 kJ mol^{-1} .^{9c}



The solid-state structures of several radical dimers of **1** ($E = S$) have been reported. For $R = Ph$, the eclipsed conformation **3** is found,^{9a} while for $R = CF_3$,^{9b} Me ,^{9c} and NMe_2 ,^{9f} the dimers adopt the twisted conformation **4** in which two rings within a cofacial pair are rotated approximately 90° about an axis through the ring centroids. In the hope of developing solid-state structures in which secondary interactions might be more pronounced, we recently extended the study of these radicals to the corresponding selenium-based systems **1** ($E = Se$).¹⁰ We found that for **1** ($E = Se$, $R = Ph$) the molecular structure of the radical dimer is eclipsed, like its sulfur counterpart, but the packing pattern is quite different; structurally significant interdimer Se-Se interactions extend along a loosely connected vertical array of dimers.

In an attempt to enhance both intra- and interstack contacts, we are now developing diradical systems in which two dithia- and diselenadiazolyl building blocks are incorporated into the same molecule. As a first step in this process we have synthesized and characterized the 1,4-phenylene-bridged diradicals **5** ($E = S$, Se). Herein we report their crystal and molecular structures and magnetic and conductivity data and discuss the results in the light of extended Hückel band structure calculations.

(9) (a) Vegas, A.; Peréz-Salazar, A.; Banister, A. J.; Hey, R. G. *J. Chem. Soc., Dalton Trans.* **1980**, 1812. (b) Hofs, H.-U.; Bats, J. W.; Gleiter, R.; Hartmann, G.; Mews, R.; Eckert-Maksić, M.; Oberhammer, H.; Sheldrick, G. M. *Chem. Ber.* **1985**, *118*, 3781. (c) Fairhurst, S. A.; Johnson, K. M.; Sutcliffe, L. H.; Preston, K. F.; Banister, A. J.; Hauptmann, Z. V.; Passmore, J. J. *Chem. Soc., Dalton Trans.* **1986**, 1465. (d) Boeré, R. T.; Oakley, R. T.; Reed, R. W.; Westwood, N. P. C. *J. Am. Chem. Soc.* **1989**, *111*, 1180. (e) Banister, A. J.; Hansford, M. I.; Hauptmann, Z. V.; Wait, S. T.; Clegg, W. *J. Chem. Soc., Dalton Trans.* **1989**, 1705. (f) Cordes, A. W.; Goddard, J. D.; Oakley, R. T.; Westwood, N. P. C. *J. Am. Chem. Soc.* **1989**, *111*, 6147. (10) Del Bel Belluz, P.; Cordes, A. W.; Kristof, E. M.; Kristof, P. V.; Liblong, S. W.; Oakley, R. T. *J. Am. Chem. Soc.* **1989**, *111*, 9276.

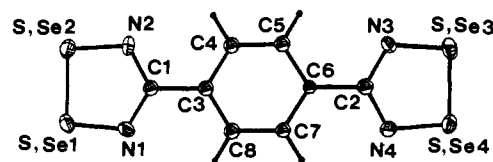
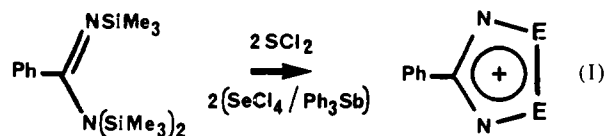


Figure 1. ORTEP drawing of **5** ($E = S$) showing atom numbering scheme. The atom numbering scheme for $E = Se$ is also shown.

Results and Discussion

Preparation of 1,4-[(E₂N₂C)₆H₄(CN₂E₂)]₂, **5 ($E = S$, Se).** There are several synthetic approaches to the 1,2,3,5-dithiadiazolium ring system.^{9b,11} The 4-phenyl derivative is commonly prepared by the reaction of benzonitrile with $S_3N_3Cl_3$,¹¹ but this method cannot be extended to the preparation of the corresponding diselenadiazolium derivative. We have found that both $[PhCN_2E_2]^+$ cations ($E = S$, Se) can be conveniently and efficiently prepared (eq 1) by condensing N,N,N' -tris(trimethylsilyl)benzamidine with either sulfur dichloride or an equimolar mixture of selenium tetrachloride and triphenylantimony (a selenium dichloride synthon¹²). The same synthetic strategy can be extended by using the 1,4-phenylene-bridged bis[N,N,N' -tris(trimethylsilyl)amidine] to generate the bis(dithiadiazolium) and bis(diselenadiazolium) dichlorides **6**. These salts are difficult to purify, as they are essentially insoluble in all organic solvents. The dications have been fully characterized, however, as their corresponding hexafluoroantimonates,¹³ which are easily generated from the dichlorides by treatment with $NOSbF_6$.



The radical dimer $[PhCN_2S_2]_2$ was first prepared by reduction of $[PhCN_2S_2]Cl$ with zinc powder in liquid sulfur dioxide.^{11b} Cyclic voltammetry on $[PhCN_2E_2]^+PF_6^-$ indicates that the selenium-based cation is reduced at a slightly (70 mV) more negative potential than the sulfur derivative.¹⁰ Both, however, are quickly and easily reduced with triphenylantimony in acetonitrile. The radical dimers are only slightly soluble in this solvent and can be isolated by filtration and purified by vacuum sublimation.

The diradical systems can likewise be generated by reduction of the corresponding dications with triphenylantimony. The crude dichlorides can be used for this purpose, but the extreme insolubility of both the starting dichlorides and product diradicals leads to rather poor yields. Reduction of the (soluble) hexafluoroantimonate salts provides an alternative route, although an extra (anion exchange) step is involved. Regardless of the starting material used, the crude diradicals are produced as black powders. Establishing a method for purification of these materials was not easy, but persistence with vacuum sublimation methods eventually proved rewarding; the sulfur compound sublimes above $160^\circ C/10^{-2}$ Torr, while the selenium derivative requires more extreme conditions, $230^\circ C/10^{-6}$ Torr. The small, black, air-stable blocks so obtained are heavily twinned, but repeated efforts eventually afforded single crystals suitable for X-ray measurements. The selenium compound **5** ($E = Se$) was also prepared as fine dendritic needles by electrochemical crystal growth from benzonitrile solutions of the corresponding dication (as its hexafluoroantimonate).

Crystal and Molecular Structures. The two diradicals **5** ($E = S$, Se) have isomorphous structures; the crystals are monoclinic,

(11) (a) Alange, G. G.; Banister, A. J.; Bell, B.; Millen, P. W. *J. Chem. Soc., Perkin Trans. I* **1979**, 1192. (b) Banister, A. J.; Smith, N. R. M.; Hey, R. G. *J. Chem. Soc., Perkin Trans. I* **1983**, 1181. (c) Apblett, A.; Chivers, T. *J. Chem. Soc., Chem. Commun.* **1989**, 96.

(12) The same effect can be achieved by using an equimolar $Se/SeCl_4$ mixture.

(13) (a) Liblong, S.; Oakley, R. T.; Cordes, A. W. *Acta Crystallogr.* **1990**, *C46*, 140. (b) Cordes, A. W.; Oakley, R. T. *Acta Crystallogr.* **1990**, *C46*, 699.

Table I. Unit Cell Data and Atomic (Non-Hydrogen) Coordinates for **5** (E = S, Se)

	$C_8H_4N_4S_4$		$C_8H_4N_4Se_4$	
<i>a</i> (Å)	5.858 (5)		5.939 (13)	
<i>b</i> (Å)	18.732 (5)		18.764 (16)	
<i>c</i> (Å)	9.340 (3)		9.569 (11)	
β (deg)	101.82 (5)		101.01 (11)	
<i>V</i> (Å ³)	1003 (2)		1047 (5)	
	<i>x</i>	<i>y</i>	<i>z</i>	<i>B</i> _{eq}
	$C_8H_4N_4S_4$			
S(1)	0.6772 (5)	0.1367 (1)	-0.0219 (3)	3.40 (6)
S(2)	0.3764 (4)	0.1320 (1)	0.0663 (3)	3.36 (6)
S(3)	1.1176 (4)	-0.2542 (1)	0.7945 (3)	3.47 (6)
S(4)	1.4219 (4)	-0.2502 (1)	0.7081 (3)	3.45 (6)
N(1)	0.811 (1)	0.0733 (4)	0.0811 (7)	3.0 (2)
N(2)	0.477 (1)	0.0670 (4)	0.1809 (7)	3.0 (2)
N(3)	0.977 (1)	-0.1963 (4)	0.6769 (7)	2.8 (2)
N(4)	1.319 (1)	-0.1918 (4)	0.5816 (8)	2.8 (2)
C(1)	0.690 (1)	0.0452 (5)	0.1737 (9)	2.3 (2) ^a
C(2)	1.099 (2)	-0.1716 (5)	0.5828 (9)	2.6 (2) ^a
C(3)	0.790 (1)	-0.0144 (5)	0.2715 (8)	2.3 (2) ^a
C(4)	0.676 (1)	-0.0376 (5)	0.3787 (9)	2.5 (2) ^a
C(5)	0.770 (1)	-0.0892 (5)	0.4774 (9)	2.5 (2) ^a
C(6)	0.987 (1)	-0.1180 (4)	0.4717 (8)	1.7 (2) ^a
C(7)	1.098 (1)	-0.0965 (5)	0.3615 (9)	2.3 (2) ^a
C(8)	1.003 (1)	-0.0433 (5)	0.2642 (9)	2.6 (2) ^a
	$C_8H_4N_4Se_4$			
Se(1)	0.6729 (6)	0.1314 (2)	-0.0319 (4)	2.70 (8)
Se(2)	0.3478 (6)	0.1283 (2)	0.0707 (4)	2.97 (8)
Se(3)	1.1045 (6)	-0.2579 (2)	0.8087 (4)	2.38 (8)
Se(4)	1.4376 (6)	-0.2544 (2)	0.7106 (4)	2.76 (8)
N(1)	0.809 (4)	0.066 (1)	0.089 (2)	1.6 (5) ^a
N(2)	0.472 (5)	0.061 (2)	0.195 (3)	2.8 (6) ^a
N(3)	0.970 (5)	-0.195 (2)	0.677 (3)	4.3 (7) ^a
N(4)	1.304 (4)	-0.191 (1)	0.583 (2)	1.7 (5) ^a
C(1)	0.685 (5)	0.046 (2)	0.179 (3)	2.2 (7) ^a
C(2)	1.089 (6)	-0.174 (2)	0.591 (3)	2.3 (7) ^a
C(3)	0.793 (5)	-0.015 (2)	0.285 (3)	3.0 (8) ^a
C(4)	0.681 (5)	-0.038 (2)	0.393 (3)	1.6 (6) ^a
C(5)	0.763 (6)	-0.088 (2)	0.485 (3)	2.5 (7) ^a
C(6)	0.986 (6)	-0.119 (2)	0.481 (3)	2.1 (6) ^a
C(7)	1.104 (6)	-0.097 (2)	0.382 (3)	2.4 (7) ^a
C(8)	1.004 (6)	-0.043 (2)	0.274 (3)	2.7 (7) ^a

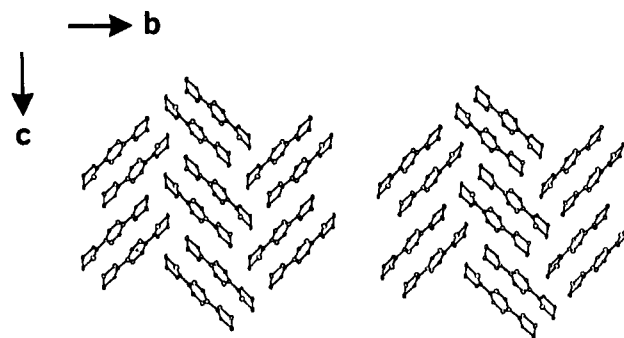
^a Atoms were refined isotropically.**Table II.** Mean Internal Structural Parameters^a for **5** and **6** (E = S, Se)^b

	E = S		E = Se	
	5	6	5	6
E-E (Å)	2.099 (9)	2.009 (4)	2.338 (19)	2.259 (12)
E-N (Å)	1.638 (22)	1.577 (9)	1.79 (3)	1.725 (19)
N-C (Å)	1.333 (14)	1.341 (14)	1.30 (9)	1.32 (7)
C-C _{exo} (Å)	1.491 (12)	1.468 (13)	1.55 (6)	1.49 (3)
N-E-E (deg)	94.4 (8)	95.5 (4)	90.6 (20)	91.1 (9)
E-N-C (deg)	114.0 (11)	115.0 (8)	114 (40)	116.8 (30)
N-C-N (deg)	123.4 (8)	119.0 (9)	131.5 (30)	124 (4)

^a Numbers in parentheses refer to the greater of the range of averaged values or the esd's for those values. ^b Values for the dication **6** are from ref 13.

space group $P2_1/n$. Unit cell data and non-hydrogen atomic coordinates for both structures are collected in Table I, and a summary of pertinent intramolecular bond length and angle information is provided in Table II. An ORTEP drawing of a single sulfur-based diradical is shown in Figure 1.

The mean internal structural parameters of the diradicals differ from those of the corresponding dication (Table II) in a predictable manner. The lengthening of the S-S and Se-Se bonds upon reduction, along with more subtle extensions in the S-N and Se-N distances collectively parallel the differences observed between the oxidation states of monofunctional derivatives. In simple MO terms, reduction of the 6π -cations to 7π -radicals results in occupation of the E-E and E-N antibonding a_2 orbital **2**. The phenyl groups show no significant differences from the dication.

**Figure 2.** Stereoview of crystal packing of **5** (E = Se). The positive *a* direction is into the page.**Table III.** Interannular E-E and E-N Contacts (Å) in **5** (E = S, Se)

	E = S		E = Se	
	E = S	E = Se	E = S	E = Se
<i>d</i> ₁	3.117 (4)	3.253 (6)	<i>d</i> ₆	4.126 (9)
<i>d</i> ₂	3.124 (4)	3.296 (6)	<i>d</i> ₇	4.010 (4)
<i>d</i> ₃	3.558 (4)	3.635 (6)	<i>d</i> ₈	3.835 (4)
<i>d</i> ₄	3.441 (4)	3.518 (6)	<i>d</i> ₉	3.990 (4)
<i>d</i> ₅	4.155 (9)	4.00 (3)	<i>d</i> ₁₀	4.105 (4)

Figure 2 illustrates a stereoview of the crystal structure of the selenium-based diradical. The dominant interannular E-E contacts for E = S and Se are indicated in Figures 3 and 4; numerical values are compared in Table III. The molecules, which are planar to within ± 0.18 Å for both E = S and Se, are packed as interleaved stacks of dimers along the *c* axis (see Figures 2 and 3). The mean intradimer separation is 3.34/3.37 Å (E = S/Se). Within each dimer, however, the two molecules are bowed in a convex manner (more so for E = S) which simultaneously maximizes the E-E contacts *d*₁ and *d*₂ (mean values are 3.121/3.275 for E = S/Se) and reduces phenyl/phenyl repulsions (the centroid-to-centroid distance is 3.53/3.45 Å for E = S/Se). Along the stacking axis the mean interplanar distance between the dimers is 3.68/3.71 Å (E = S/Se). The interlocking nature of the dimer units also produces close "perpendicular" contacts between radical units; the mean of the E-E contacts *d*₃ and *d*₄ is 3.500/3.578 Å (E = S/Se). All the distances *d*₁-*d*₄ are well within the respective van der Waals' separations¹⁴ for sulfur (3.6 Å) and selenium (3.8 Å), those between the cofacial rings being similar to the intradimer separations in [PhCN₂S₂]₂ (mean *d*(S-S) = 3.105 Å) and [PhCN₂Se₂]₂ (mean *d*(Se-Se) = 3.253 Å). There are also relatively close, although clearly beyond, van der Waals E-N contacts (mean of *d*₅ and *d*₆) of 4.141/3.98 Å (E = S/Se) which arise from the close approach of two radical rings in a head-over-tail fashion (see Figure 3). This kind of overlap has not been observed for monofunctional radicals **1**.

Figure 4 provides a perspective of the packing (for E = Se), which highlights the nearly orthogonal disposition of the dimers along the stacking backbone, and also shows the four close E-E contacts *d*₇-*d*₁₀ (see Table III) between the sheets of dimers. For E = Se these contacts are similar in magnitude to the intercolumnar contacts seen in TMTSF salts,³ while for E = S the contacts lie outside the van der Waals range.

ESR Spectra. Solution-based ESR spectral parameters have been reported for a wide range of dithiadiazolyls **1** (E = S); *g* values are characteristically near 2.01, and hyperfine splitting constants to nitrogen (*a*_N) are almost invariant at a value near 0.50 mT.^{9b-d,f} The room temperature ESR spectrum of **1** (E = Se, R = Ph) has also been reported. The *g* value (2.0394) is predictably larger,¹⁰ approaching the values seen in [Sn₂Se₂]^{•+} and [SeN₂Se₂]^{•+},¹⁵ and anisotropy in the *g* value leads to a complete loss of resolution of hyperfine coupling to nitrogen. ESR

(14) Bondi, A. *J. Phys. Chem.* **1964**, *68*, 441.(15) (a) Awere, E. G.; Passmore, J.; Preston, K. F.; Sutcliffe, L. H. *Can. J. Chem.* **1988**, *66*, 1776. (b) Awere, E. G.; Passmore, J.; White, P. S.; Klaptke, T. *J. Chem. Soc., Chem. Commun.* **1989**, 1415.

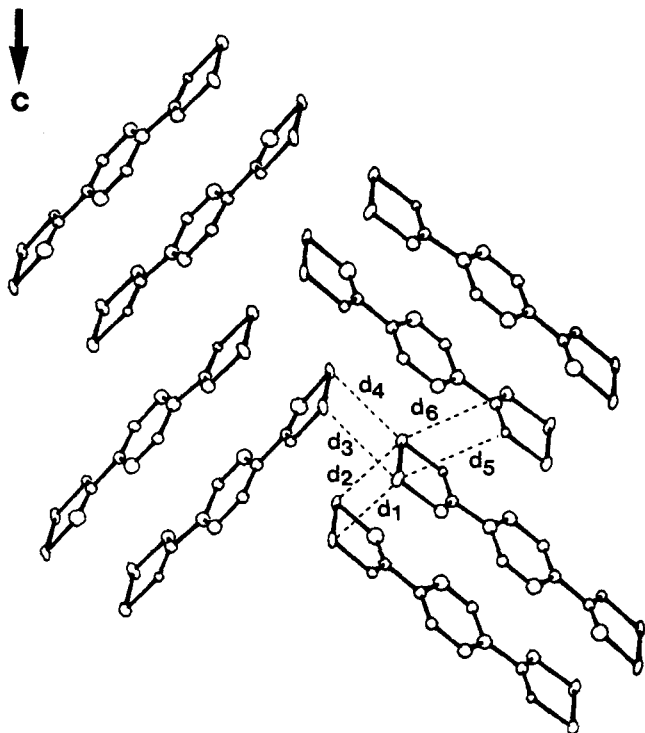


Figure 3. Definition of intermolecular contacts d_1 - d_6 . The positive a direction is into the page.

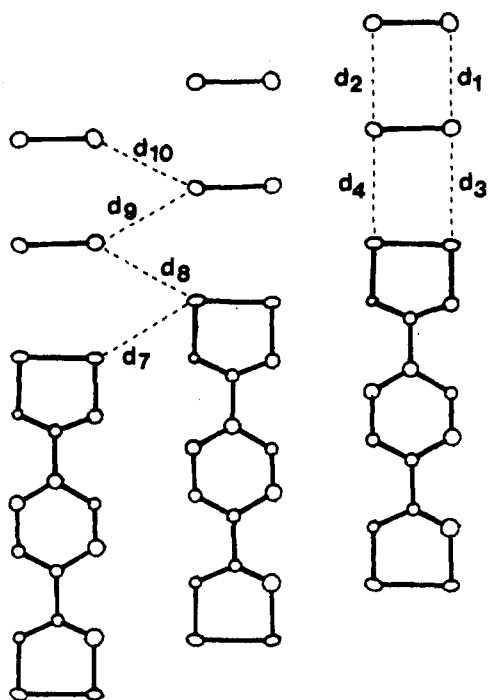


Figure 4. Definition of intermolecular contacts d_7 - d_{10} . The left hand molecules are above, and the right molecules are below the plane of the paper. The center molecules lie in the plane of the paper.

data for the diradical species described here is limited to $E = S$; for $E = Se$ the solid is sufficiently insoluble to reduce signal intensity below the detection limit. The ESR signal $\mathbf{5}$ ($E = S$), recorded on a saturated solution in chloroform, has a g value of 2.011. As illustrated in Figure 5, the spectrum shows a temperature dependence characteristic of very weak intramolecular¹⁶ exchange coupling (J_{ex}) between two radical centers.¹⁷ At -60

(16) The low solubility of the diradicals precludes any possibility of intermolecular exchange interactions.

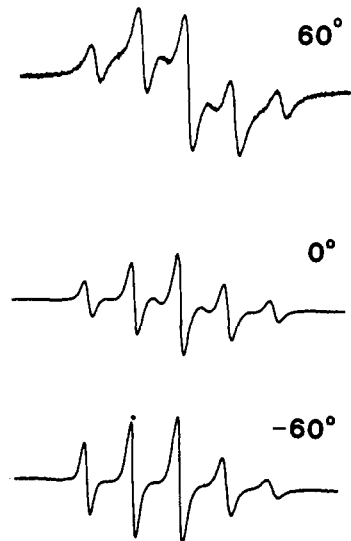


Figure 5. ESR spectrum of $\mathbf{5}$ ($E = S$) in $CHCl_3$ at different temperatures ($^{\circ}C$).

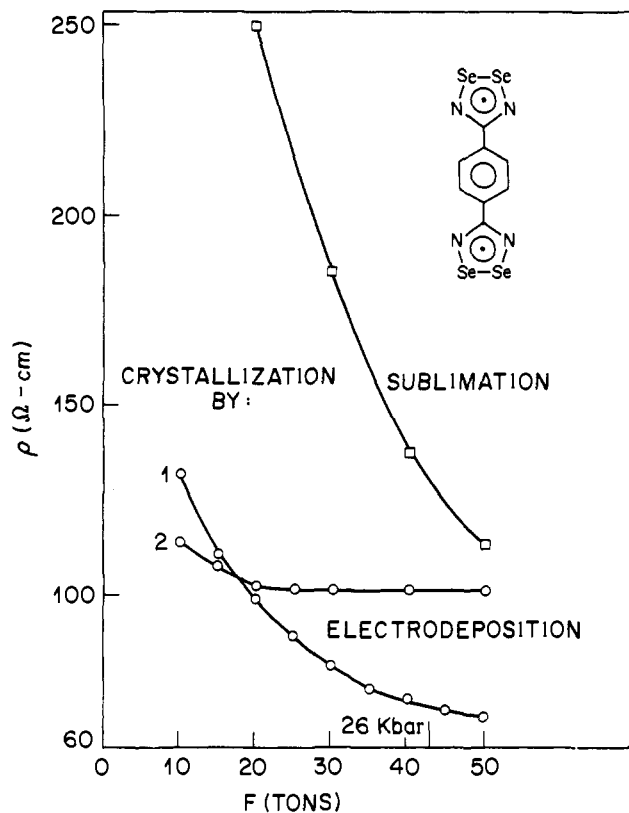


Figure 6. Room temperature conductivity of $\mathbf{5}$ ($E = Se$) prepared by both sublimation and electrodeposition. Results for two electrodeposition samples (1 and 2) are shown.

$^{\circ}C$ the spectrum is that expected for noninteracting radical centers, i.e., a simple five-line pattern with $a_N = 0.51$ mT. Above this temperature the spectrum begins to reveal the influence of exchange coupling between the two radical centers. Qualitatively these features are consistent with a high-temperature limit in which $J_{ex} > a_N$. The origin of the temperature dependence is unclear; rotational motion about the ring-connector C-C bonds may be important in aligning the three rings of $\mathbf{5}$, as may be the effect

(17) (a) Glarum, S. H.; Marshall, J. H. *J. Chem. Phys.* **1967**, *47*, 1374. (b) Briere, P.; Dupuyre, R.-M.; Lemaire, H.; Morat, C.; Rassat, A.; Rey, P. *Bull. Chim. Soc. Fr.* **1965**, 3290. (c) Reitz, D. C.; Weissman, S. I. *J. Chem. Phys.* **1960**, *33*, 700. (d) Eaton, G. R.; Eaton, S. S. *Acc. Chem. Res.* **1988**, *21*, 107.

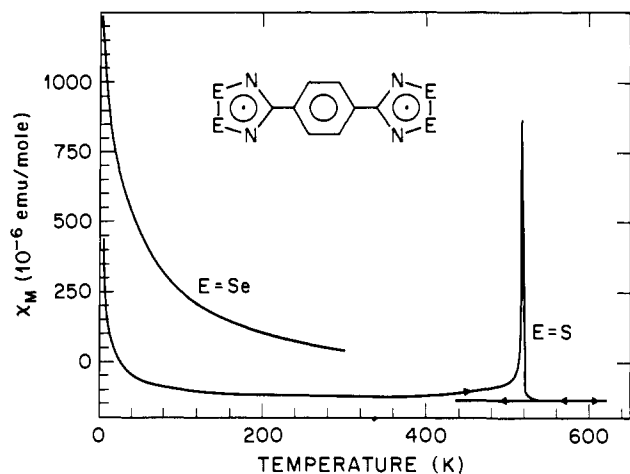


Figure 7. Variable temperature magnetic susceptibility of **5** (E = S and Se).

of solvent (on solvent-assisted through-space exchange). Additional studies on a wider range of diradicals of this type will be required to understand the mechanism of exchange.

Conductivities. The room temperature conductivity for the selenium compound (**5**, E = Se) as a function of pressure under quasi-hydrostatic conditions is shown in Figure 6. Under the same conditions the sulfur compound (**5**, E = S) proved to be an insulator at all accessible pressures. The results shown in Figure 6 are pressed pellet measurements, as it has not yet been possible to produce material suitable for single crystal measurements. There is no evidence for a pressure dependence for the intrinsic conductivity, and we ascribe the variation to the improved packing of the crystallites at higher pressures. The band structure calculations (discussed below) suggest that these materials are semiconductors, but without conductivities as a function of temperature it is not possible to assign the origin of the conductivity in this material. The sample variations (Figure 6) suggest that the mode of preparation of the compound is important, and this may indicate that the material is not displaying intrinsic conductivity. Although the preparations analyze correctly for the composition, the conductivity of semiconductors is extremely sensitive to the presence of trace impurities or defects.¹⁸

Magnetic Susceptibilities. The magnetic susceptibilities as a function of temperature are shown in Figure 7. It may be seen that both species show a predominantly low-temperature Curie behavior, although the paramagnetism arises from a small fraction of the sample. A Curie-Weiss fit to the low-temperature magnetic susceptibility data of the sulfur compound gives a θ value of 5 K and a spin concentration of 1% on a molecule basis, whereas the selenium compound showed a larger paramagnetism, particularly with material which was sublimed more quickly. The sample (E = Se), which was measured for Figure 8, gave a θ value of 58 K and a spin concentration of 16% on a molecule basis.

After subtraction of the Curie contribution, the samples are predominantly diamagnetic; this amounts to -140 (E = S) and -130 (E = Se) ppm emu/mol. By using a recent compilation¹⁹ of Pascal's constants, we estimate molecular diamagnetic susceptibilities of -147 (E = S) and -179 (E = Se) ppm emu/mol. These results suggest that the pristine crystalline material is diamagnetic but that there is a variable amount of paramagnetic defects in the lattice, presumably corresponding to monomeric radical sites. These defects may also provide the carriers associated with the conductivity of the selenium material.

In the high-temperature regime of the sulfur compound, there is a large enhancement at the melting/decomposition point of the compound, and it seems likely that this is associated with the dissociation of the dimers just before sample decomposition.

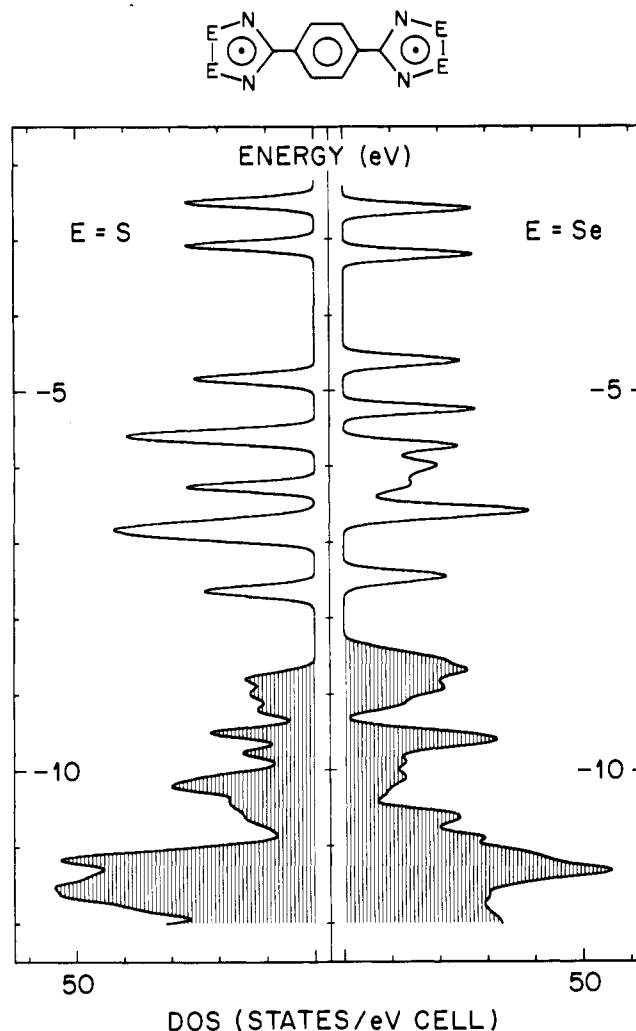


Figure 8. Calculated density of states of crystalline **5** (E = S and Se).

Band Structure Calculations. The calculated density of states for the two crystal structures are given in Figure 8. The calculations were carried out with a reparameterized version of the Extended Hückel theory band structure program (calculational section).

The calculations show that the dimerization opens up a gap in the density of states for both compounds; they are predicted to be semiconductors with $E_g = 0.84$ eV (E = S) and 0.69 eV (E = Se). The calculated band dispersions for the highest occupied and lowest unoccupied bands along the principal directions are shown in Figure 9. The band dispersions are quite moderate by the standards of most conducting organic charge transfer salts, which typically show values of the order of 0.5 eV. Perhaps of most interest is the degree of anisotropy of these materials. Even though there is a pseudostacking axis in this material, the band structures indicate that the crystals are relatively isotropic. The dispersions in the *B* and *Z* directions (Figure 9) are the largest and are of comparable magnitude. The dispersion along *Y* is about a factor of 5 smaller. Nevertheless, these compounds are, to our knowledge, the most three-dimensional organic molecular solids yet to be reported. For example, the ratios of the transfer integrals in (TMTSF)₂ClO₄ have been reported²⁰ as 300:30:1, whereas κ -(BEDT-TTF)₂Cu(NCS)₂ is almost isotropic in two dimensions, but with very little interaction in the third direction.²¹

The directions of largest dispersion in crystalline **5** lie along a^* and c^* and correspond to a composite of the contact between

(18) Schwarz, S. A. *Encyclopedia of Semiconductor Technology*; J. Wiley: New York, 1984; p 699.

(19) Carlin, R. L. *Magnetochemistry*; Springer-Verlag: Berlin, 1986; p 3.

(20) Poilblanc, D.; Montambaux, G.; Heritier, M.; Lederer, P. *Phys. Rev. Lett.* **1987**, *58*, 270.

(21) (a) Saito, G. *Physica* **1989**, C162-164, 577. (b) Kanoda, K.; Takahashi, T.; Saito, G. *Physica* **1989**, C162-164, 405.

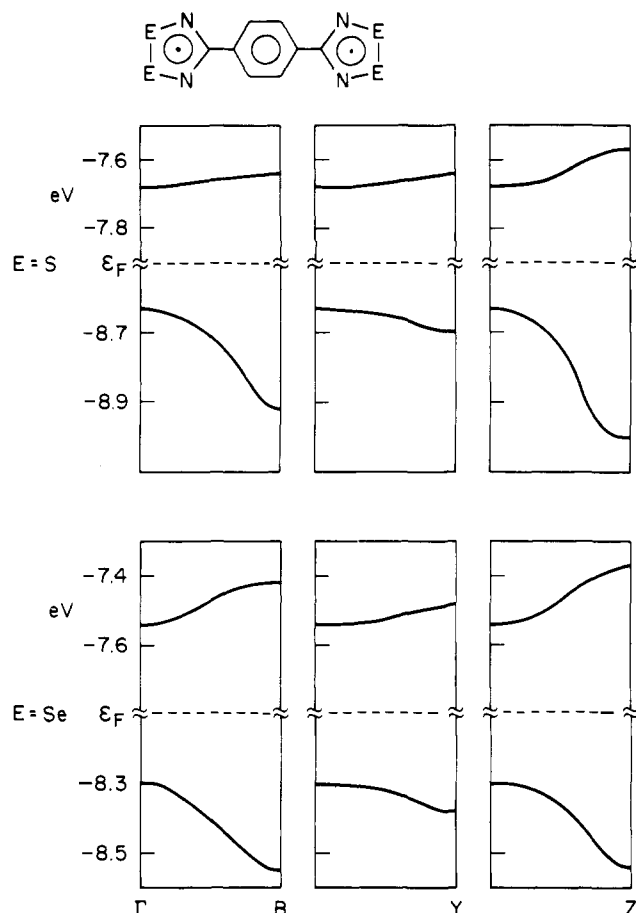


Figure 9. Dispersion relations of the highest occupied and lowest unoccupied bands of crystalline **5** ($E = S$ and Se) along the principal directions in reciprocal space, where $\Gamma = (0,0,0)$, $B = (a^*/2,0,0)$, $Y = (0,b^*/2,0)$, $Z = (0,0,c^*/2)$, and ϵ_F is the Fermi level.

the stacks as seen in Figure 4 and the interaction along the stacking axis (Figure 3). The weak interaction along b^* (collinear with b) corresponds to the overlap between adjacent stacks of molecules which lie at right angles to one another as shown in Figure 3.

Summary and Conclusions. The solid-state structures of 1,4-phenylene-bridged bifunctional dithia- and diselenadiazolyl radicals reveal a complex network of interrational contacts. The extent of dimerization, and hence electron localization, is more pronounced in the sulfur compound and gives rise to a completely insulating ground state. In the selenium derivative, interactions lead to a more three-dimensional electronic structure and a reduced band gap; the moderate conductivity exhibited by this system can be understood in these terms. While the exact mechanism of conduction remains to be established, these systems represent the first structurally characterized conducting material constructed from neutral molecular radicals.

Experimental Section

Starting Materials and General Procedures. Benzonitrile, 1,4-dicyanobenzene, lithium bis(trimethylsilyl)amide, sulfur dichloride, selenium powder, nitrosyl hexafluoroantimonate, and triphenylantimony were all obtained commercially (Aldrich). Sulfur dichloride was distilled before use. Benzonitrile was purified by vacuum distillation from P_2O_5 . Acetonitrile (Fisher HPLC grade) was also purified by distillation from P_2O_5 . All reactions were performed under an atmosphere of nitrogen. N,N,N' -Tris(trimethylsilyl)benzamidine (BADS), 1,4-phenylenebis(N,N,N' -tris(trimethylsilyl)amidine) (1,4-DIBADS),²² and selenium tetrachloride²³ were all prepared according to literature methods. Mass spectra were recorded on a Kratos MS890 mass spectrometer. ESR spectra were recorded with a Varian E-109 spectrometer on samples

dissolved in chloroform (predried over P_2O_5); solutions were degassed by a series of at least five freeze/pump/thaw cycles. Infrared spectra (CsI optics, Nujol mulls) were obtained on a Nicolet 20SX/C FTIR instrument. Elemental analyses were performed by MHW Laboratories, Phoenix, AZ. High vacuum (pressures $\leq 10^{-6}$ Torr) sublimations were performed with an Edwards ETP200 Turbomolecular pump backed by an Edwards E2M8 two-stage mechanical pump.

Preparation of $[PhCN_2S_2]Cl$.²⁴ Solid BADS (1.82 g, 5.4 mmol) was added through a powder funnel to a solution of SCl_2 (2.0 mL, excess) in 50 mL of acetonitrile, and the resulting mixture was stirred and heated to near 60 °C for 1 h. The mixture was then cooled to 0 °C and filtered to afford $[PhCN_2S_2]Cl$ (1.06 g, 5.0 mmol, 90%). The identity of this material was confirmed by comparison of its infrared spectrum with literature data.^{11a}

Preparation of $[PhCN_2Se_2]Cl$. A solution of BADS (1.78 g, 5.0 mmol) and Ph_3Sb (3.53 g, 10.0 mmol) in 15 mL of acetonitrile was added dropwise to a slurry of $SeCl_4$ (2.20 g, 10.0 mmol) in 40 mL of acetonitrile. The mixture was heated to 60 °C for 30 min and then cooled to room temperature, and the orange/brick red precipitate so formed was collected by filtration. The product $[PhCN_2Se_2]Cl$ (1.4 g, 4.6 mmol, 91%) was only sparingly soluble in acetonitrile but could be recrystallized for analytical purposes from this solvent to give fibrous orange needles, dec > 180 °C: IR (1600–250- cm^{-1} region) 1448 (m), 1344 (s), 1133 (w), 1025 (w), 790 (w), 778 (m), 746 (m), 699 (s), 692 (s), 677 (w), 445 (w), 432 (w) cm^{-1} . Anal. Calcd for $C_7H_5N_2Se_2Cl$: C, 27.08; H, 1.62; N, 9.02; Cl, 11.42. Found: C, 26.77; H, 2.16; N, 8.66; Cl, 11.70.

Preparation of $[PhCN_2Se_2]_2$. Solid Ph_3Sb (0.80 g, 2.3 mmol) was added to a slurry of $[PhCN_2Se_2]Cl$ (1.40 g, 0.45 mmol) in 50 mL of acetonitrile. The mixture was stirred rapidly at 60 °C for 1 h and then cooled to room temperature, and the sparkling black microcrystals (dec > 180 °C) of $[PhCN_2Se_2]_2$ (1.05 g, 1.9 mmol, 87%) were isolated by filtration. The dimer was purified by sublimation at 100 °C/ 10^{-2} Torr: IR (1600–250- cm^{-1} region) 1489 (w), 1447 (m), 1377 (w), 1326 (m), 1311 (m), 1269 (w), 1111 (w), 1027 (w), 768 (m), 734 (w), 715 (s), 698 (s), 686 (s), 652 (s), 612 (m), 425 (m) cm^{-1} . Anal. Calcd for $C_{14}H_{10}N_4Se_4$: C, 30.57; H, 1.83; N, 10.18. Found: C, 30.89; H, 1.87; N, 10.14.

Preparation of 1,4- $[(S_2N_2C)C_6H_4(CN_2S_2)]X_2$ ($X^- = Cl^-, SbF_6^-$). Solid 1,4-DIBADS (5.95 g, 10.0 mmol) was added to a solution of SCl_2 (5 mL, excess) in 100 mL of acetonitrile. The resulting mixture was heated at gentle reflux for 2 h and then filtered to afford 1,4- $[(S_2N_2C)C_6H_4(CN_2S_2)]Cl_2$ (3.3 g, 9.3 mmol, 93%) as an orange granular solid [IR (1600–250- cm^{-1} region) 1377 (s), 1161 (m), 1022 (w), 889 (m), 844 (s), 701 (s), 538 (s) cm^{-1}]. The crude chloride salt (1.02 g, 2.9 mmol) was converted into the corresponding hexafluoroantimonate by treatment with $NOSbF_6$ (1.7 g, 6.6 mmol) in 20 mL of benzonitrile. Crystallization from hot benzonitrile afforded bright yellow crystals of 1,4- $[(S_2N_2C)C_6H_4(CN_2S_2)][SbF_6]_2 \cdot 2PhCN$ (1.8 g, 1.9 mmol, 65%). Anal. Calcd for $C_{22}H_{14}N_6S_4Sb_2F_6$: C, 27.46; H, 1.47; N, 8.73. Found: C, 27.27; H, 1.27; N, 8.68. The composition of this material has been confirmed by X-ray crystallography.^{13a}

Preparation of 1,4- $[(Se_2N_2C)C_6H_4(CN_2Se_2)]X_2$ ($X^- = Cl^-, SbF_6^-$). A mixture of solid Ph_3Sb (14.12 g, 40.0 mmol) and 1,4-DIBADS (5.95 g, 10.0 mmol) was added through a powder funnel to a slurry of $SeCl_4$ (8.84 g, 40 mmol) in 125 mL of CH_3CN . This mixture was heated to reflux for 5 h, then cooled, and filtered to yield 4.8 g (8.8 mmol, 88%) of crude 1,4- $[(Se_2N_2C)C_6H_4(CN_2Se_2)]Cl_2$ as a brick red powder [IR (1600–250- cm^{-1} region) 1360 (m), 1340 (s), 1136 (m), 1017 (m), 851 (w), 783 (m), 732 (s), 687 (s), 414 (m) cm^{-1}]. The crude chloride salt (4.8 g, 8.8 mmol) was converted into the corresponding hexafluoroantimonate by treatment with $NOSbF_6$ (5.0 g, 18.9 mmol) in 60 mL of benzonitrile. Crystallization from hot benzonitrile afforded bright yellow crystals of 1,4- $[(Se_2N_2C)C_6H_4(CN_2Se_2)][SbF_6]_2 \cdot 3PhCN$ (5.3 g, 4.2 mmol, 48%). Anal. Calcd for $C_{29}H_{19}N_7Se_4Sb_2F_{12}$: C, 27.80; H, 1.53; N, 7.83. Found: C, 26.90; H, 1.43; N, 7.46. The composition of this material has been confirmed by X-ray crystallography.^{13b}

Preparation of 1,4- $[(S_2N_2C)C_6H_4(CN_2S_2)]_2$. Solid Ph_3Sb (3.5 g, 10.0 mmol) was added to a slurry of crude 1,4- $[(S_2N_2C)C_6H_4(CN_2S_2)]Cl_2$ (3.3 g, 9.4 mmol) in 100 mL of acetonitrile, and the mixture was stirred rapidly and heated to about 60 °C for 2 h. The black precipitate was filtered off and dried in vacuo. This crude product (2.6 g), which is quite sensitive to oxygen, was then slowly sublimed (over several days) at 175–80 °C/ 10^{-2} Torr to afford small, black, air-stable blocks of 1,4- $[(S_2N_2C)C_6H_4(CN_2S_2)]_2$ (0.84 g, 0.3 mmol, 32% based on crude dichloride, dec > 310 °C: IR (1600–250- cm^{-1} region) 1418 (w), 1368 (s), 1182 (w), 1150 (w), 1128 (m), 1112 (w), 1020 (w), 855 (m), 837 (w),

(22) Boeré, R. T.; Oakley, R. T.; Reed, R. W. *J. Organomet. Chem.* **1987**, *331*, 161.

(23) Brauer, G. *Handbook of Preparative Chemistry*; Academic: New York, 1963; Vol. 1, p 423.

(24) A variation (with lower yield) of this procedure has recently been reported. See: Amin, A.; Rees, C. W. *J. Chem. Soc., Perkin Trans. I* **1989**, 2495.

Table IV. Parameters for Extended Hückel Theory Calculations^a

atom	orbital	H_{ii} (eV)	C_1	ζ_1	C_2	ζ_2
H	1s	-13.6	1.0	1.3		
C	2s	-19.4	0.7616	1.831	0.2630	1.153
	2p	-10.6	0.2595	2.730	0.8025	1.257
N	2s	-25.6	0.6978	2.261	0.3304	1.425
	2p	-13.2	0.2881	3.249	0.7783	1.499
S	3s	-20.7	0.5564	2.662	0.4873	1.688
	3p	-11.6	0.5212	2.338	0.5443	1.333
Se	4s	-20.8	0.5830	3.139	0.4852	1.890
	4p	-10.8	0.5347	2.715	0.5553	1.511

^aThe coulomb parameters (H_{ii}) are taken from ref 28. A single STO is employed for hydrogen together with the standard Slater exponent. The basis sets for the valence orbitals of the other atoms are a contraction of the split-valence basis sets given in ref 31 (see also ref 30).

827 (w), 802 (s), 775 (s), 658 (s), 504 (m), 412 (w), 368 (w) cm^{-1} ; mass spectrum (EI, 40 eV, m/e) 284 (100, M^+), 238 (25, $(\text{M} - \text{SN})^+$), 206 (63, $(\text{M} - \text{S}_2\text{N})^+$), 128 (20, $(\text{NCC}_6\text{H}_4\text{CN})^+$), 78 (52, S_2N^+), 64 (10, S^{2+}). Anal. Calcd for $\text{C}_8\text{H}_4\text{N}_4\text{S}_4$: C, 33.19; H, 1.42; N, 19.70; S, 45.09. Found: C, 33.90; H, 1.25; N, 19.74; S, 44.86.

Preparation of 1,4-[($\text{Se}_2\text{N}_2\text{C}$) $\text{C}_6\text{H}_4(\text{CN}_2\text{Se}_2)$]. Solid Ph_3Sb (2.1 g, 6.0 mmol) was added to a slurry of 1,4-[($\text{Se}_2\text{N}_2\text{C}$) $\text{C}_6\text{H}_4(\text{CN}_2\text{Se}_2)$] Cl_2 (2.71 g, 5.0 mmol) in 100 mL of acetonitrile, and the mixture was stirred rapidly and heated to 60 °C for about 2 h. The black precipitate was filtered off and dried in vacuo. This crude product (2.2 g) was purified (in small quantities) by slow sublimation (over several days) at 230 °C/ 10^{-6} Torr to yield small black (gold to reflected light) blocks of 1,4-[($\text{Se}_2\text{N}_2\text{C}$) $\text{C}_6\text{H}_4(\text{CN}_2\text{Se}_2)$], mp > 350 °C. Yields of sublimed material were normally near 20%: IR (1600–250- cm^{-1} region) 1316 (m), 1307 (sh), 1264 (w), 1176 (w), 1135 (w), 1111 (m), 1016 (w), 855 (m), 710 (s), 696 (s), 612 (m), 397 (m) cm^{-1} ; mass spectrum (EI, 20 eV, m/e) 474 (26, multiplet, Se_6^+), 302 (48, multiplet, $(\text{M} - \text{Se}_2\text{N})^+$), 174 (14, multiplet, Se_2N^+), 160 (100, multiplet, Se_2^+), 128 (100, $(\text{NCC}_6\text{H}_4\text{CN})^+$). (The appearance of Se_6^+ in the mass spectrum is attributed to considerable sample decomposition on the probe.) Anal. Calcd for $\text{C}_8\text{H}_4\text{N}_4\text{Se}_4$: C, 20.36; H, 0.85; N, 11.87. Found: C, 20.40; H, 0.81; N, 11.74.

Electrocrystallization of 5 (E = Se). Small quantities of fine, heavily twinned needles of 5 (E = Se) were also obtained by electrocrystallization onto indium tin oxide electrodes from solutions of 1,4-[($\text{Se}_2\text{N}_2\text{C}$) $\text{C}_6\text{H}_4(\text{CN}_2\text{Se}_2)$] $[\text{SbF}_6]_2 \cdot 3\text{PhCN}$ (100–200 mg) in 50 mL of PhCN at 80–100 °C. No supporting electrolyte was used, and the solution was simply partitioned between the two halves of a standard H-cell. Crystals were grown over 24–48 h under constant current (20–50 μA) conditions.

X-ray Measurements. Crystals of 5 (E = S, Se) suitable for single crystal X-ray work were grown by slow sublimation as described above. All X-ray data were collected on an ENRAF-Nonius CAD-4 at 293 K with monochromated $\text{Mo K}\alpha$ ($\lambda = 0.71073$ Å radiation). Crystals were mounted on glass fibers coated with epoxy. Data were collected by using a $\theta/2\theta$ technique with a scan width of $(1.0 + 0.3 \tan \theta)$. Both structures were solved by using MULTAN and refined by full-matrix least squares which minimized $\sum w(\Delta F)^2$. Data collection, structure solution, and refinement parameters for both structures are available as supplementary material. Crystals of both 5 (E = S and Se) were prone to twin, leading to a lack of long-range order and weak high angle reflections. In the case of E = Se the data set used was the best of seven sets collected. The relatively high R (0.044 for E = S, 0.062 for E = Se) and R_w (0.050 for E = S, 0.072 for E = Se) values and bond esd's are a result of a paucity of high angle data and a resultant inability to perform a full anisotropic refinement; for E = S all C atoms were refined isotropically, and for E = Se both N and C atoms were refined isotropically.

Conductivity Measurements. Conductivities were measured in a Bridgman anvil cell using isomica washers to contain the sample. The

resistance between the pole faces was used to calculate the conductivity after correction for the sample geometry. Pressure was applied with a hydraulic press of 50 ton capacity. The cell was calibrated with a standard bismuth sample which showed the characteristic feature in the resistivity at 26 kbar.²⁵ The resistivity in the selenium compound showed some hysteresis as a function of pressure; the results shown in Figure 6 are the final curves after cycling the cell between 0 and 50 tons of applied pressure. R.C.H. and N.M.Z. are grateful to A. Jayaraman and R. G. Maines for use of their pressure equipment.

Magnetic Susceptibility Measurements. The magnetic susceptibility was measured from 4.2 to 650 K by using the Faraday technique. Details of this apparatus have been previously described.²⁶ The applied field was 14 kOe, and the measured susceptibility was checked for field dependence at several temperatures.

Band Structure Calculations. The band structures were carried out with the EHMACC suite of programs which was supplied to R.C.H. by M.-H. Whangbo, and we are grateful to him for many discussions on the use of this program and to G. W. Trucks for assistance in adapting the code to the local machines at AT&T Bell Laboratories. We found the standard version of the program to be unsatisfactory for comparisons between conjugated sulfur–nitrogen and selenium–nitrogen heterocycles.²⁷ We therefore adopted the set of coulomb parameters given by Basch, Viste, and Gray²⁸ (Table IV). Although these parameters may not represent the best choice in every situation, we felt that internal consistency was the most important criterion in parameter selection. The off-diagonal elements of the Hamiltonian matrix were calculated with the standard weighting formula.²⁹

Following Whangbo and co-workers³⁰ we used a quasi-split valence basis set, using the expansion given by Clementi and Roetti³¹ (Table IV), as this basis provides a better description of the weak interactions which are characteristic of organic molecular solids. The density of states were obtained by taking points in the irreducible Brillouin zone according to the sampling scheme given by Bohm and Ramirez.³² The chosen grid in k space gave rise to 30 points which are listed in the supplementary material.

Acknowledgment. Financial support at Guelph was provided by the Natural Sciences and Engineering Research Council of Canada and at Arkansas by the National Science Foundation (EPSCOR program) and the State of Arkansas. R.C.H. acknowledges valuable discussions with D. W. Murphy, S. H. Glarum, B. Golding, P. B. Littlewood, T. T. M. Palstra, A. P. Ramirez, and G. W. Trucks.

Supplementary Material Available: Tables of crystal data, structure solution, and refinement (S1), H-atom coordinates (S2), bond lengths and angles (S3), anisotropic thermal parameters (S4) for 1,4-[($\text{E}_2\text{N}_2\text{C}$) $\text{C}_6\text{H}_4(\text{CN}_2\text{E}_2)$] (E = S, Se), and reciprocal space points (S5) (7 pages). Ordering information is given on any current masthead page.

(25) Andersson, G.; Sundqvist, B.; Bäckström, G. *J. Appl. Phys.* **1989**, *65*, 3943.

(26) (a) DiSalvo, F. J.; Waszczak, J. V. *Phys. Rev.* **1981**, *B23*, 457. (b) DiSalvo, F. J.; Menth, A.; Waszczak, J. V.; Tauc, J. *Phys. Rev.* **1972**, *B6*, 4574.

(27) See ref 7 for a discussion of the Hückel parameterization of S and N in SN rings.

(28) Basch, H.; Viste, A.; Gray, H. B. *Theor. Chim. Acta* **1965**, *3*, 458.

(29) Ammeter, J. H.; Burghi, H. B.; Thibeault, J. C.; Hoffman, R. *J. Am. Chem. Soc.* **1978**, *100*, 3686.

(30) Emge, T. J.; Wang, H. H.; Beno, M. A.; Williams, J. M.; Whangbo, M.-H.; Evain, M. *J. Am. Chem. Soc.* **1986**, *108*, 8215.

(31) Clementi, E.; Roetti, C. *At. Data Nucl. Data Tables* **1974**, *14*, 177.

(32) Ramirez, R.; Bohm, M. C. *Int. J. Quant. Chem.* **1988**, *34*, 571.